Quality by Design Approach for Fabrication of Rifampicin-Loaded Solid Lipid Nanoparticles: Effect on Formulation and Characteristic Parameters

Bibhash C. Mohanta[1], Subas C. Dinda[2], Narahari N. Palei[3], Gitanjali Mishra[4]

[1]School of Pharmaceutical Education and Research, Berhampur University, Ganjam, Odisha, India, [2]Department of Pharmaceutics, College of Pharmacy, Teerthanker Mahaveer University, Moradabad, Uttar Pradesh, India, [3]Department of Pharmaceutics, Sree Vidyanikethan College of Pharmacy, Tirupati, Andhra Pradesh, India, [4]Department of Zoology, Berhampur University, Ganjam, Odisha, India

Abstract

Introduction: Rifampicin (RIF), a first-line anti-tuberculosis drug having an inimitable potential of rapidly killing mycobacterium. Unfortunately, it has poor bioavailability, short half-life period ($t_{1/2}$), and intense toxicity. To solve the problem, solid lipid nanoparticles (SLN) of RIF were developed by high-pressure homogenization followed by ultrasonication technique. **Objectives:** The objective of this work was to understand the process variables and their effect on formulation aspects through an experimental approach and to optimize the formulation with the application of response surface methodology. **Materials and Methods:** The quality by design of $3^{(2)}$ factorial was employed for the optimization of the formulation. The concentration of stearic acid (SA), lecithin, and poloxamer (POL) was considered as an independent factor, and their impact on particle size (PS), entrapment efficiency (%EE), and cumulative drug release (%CDR) was investigated. **Results and Discussion:** It was found that SA and lecithin had a positive impact, but POL had a negative impact on PS and %EE. The %CDR was positively influenced by lecithin and POL concentration, whereas it was negatively influenced by SA concentration. The average PS, zeta potential, and %EE of the optimized formulation were found to be 172.5 nm, −025.6 mV, and 70.34%, respectively. The optimized formulation showed a %CDR of 64.34% in 96 h, and the drug release pattern followed non-Fickan kinetics. X-ray diffraction study revealed large amorphousness nature of RIF in SLNs. Scanning electron microscopy study reported spherical shaped nanometric size particles. It was revealed from the stability study that the developed RIF-SLNs were stable at $4 \pm 2°C$ when compared with their storage at $25 \pm 2°C/60 \pm 5\%$ RH in 6 months of storage period. **Conclusions:** These results implied that the prepared RIF-SLNs could improve bioavailability and reduce toxicity for effective tuberculosis therapy.

Key words: Characterization, *in vitro* release, quality by design, response surface methodology, rifampicin, solid lipid nanoparticles

INTRODUCTION

Tuberculosis (TB) is attributable to *Mycobacterium* TB (MTb), which is an epidemic disease of the respiratory system. It represents one of the major health threats to human population, distressing up to 33% of the total global population.[1] As per the World Health Organization's, "Global TB report 2017," in 2016, about 1.3 million died due to TB occurred across the globe. In addition, 370,000 deaths were resulting from coinfection of TB with HIV.[2]

Rifampicin (RIF), a first-line anti-tuberculosis drug (ATD) having an inimitable potential of

killing the MTb by inhibiting the DNA-dependent RNA polymerase resulting in curbing the initiation of RNA synthesis.[3] Unfortunately, RIF endure from poor and erratic bioavailability, short half-life ($t_{1/2}$) period, high

hepatic clearance, intestinal metabolism, and intense hepatotoxicity that restrict its use.[4] Numerous attempts were made to develop a variety of novel dosage forms of RIF, including microspheres,[5] liposomes,[6] and nanoparticles[4,7] for improvement of bioavailability, reduction in toxicity, and better patient compliance for ATDs.

Since the induction of nanotechnology in drug delivery system in 1972, numerous formulations such as nanoparticles, nanosuspensions, nanoemulsion, niosomes, and liposomes have been suggested to achieve satisfactory therapeutic efficacy through improvement of oral bioavailability and reduction of the toxicity. However, the last three decades ago, lipid-based nanoparticles were introduced as an alternative to polymeric nanoparticles, as they have the ability to eliminate most of the limitations associated with the later. Solid lipid nanoparticles (SLNs), the second-generation lipid-based nanocarriers[8] are recently gaining much more attention due to their innate characteristics such as physicochemical diversity, biocompatibility and biodegradability, improved bioavailability, ability to incorporate both nonpolar and polar drug with higher drug incorporating efficiency, and controlled release characteristics.[9] As a drug delivery system, SLNs play a significant role in delivering ATDs such as RIF. MTb possesses a special range of lipases that have a strong affinity for lipidic substrate. Thus, lipidic nature of SLNs may magnetize the MTb.[10] The mycobacterium lipase acts on RIF-SLNs that induce the release of RIF from SLN to the close vicinity of the MTb ensuing in a much rapid and superior antimicrobial effect.[11] Moreover, due to its nano-size, the SLNs may enter inside to the macrophage resulting in localization of higher concentration of drugs at the site where most of the mycobacterium reside.

Recently, the statistical experimental design quality by design (QbD) is considered as an essential tool for fabricating the optimized formulations in various drug delivery systems when complicated interaction is taking place between various process variables. It also provides better understanding of the relationship between the independent and the dependent variables through response surface methodology (RSM).[12] This study has used QbD (2^3 full factorials) design-RSM tool for process optimization.

The objectives of this study were to investigate and to screen the detailed impact of formulation process variables affecting the quality and characteristics of RIF-SLNs through the statistical approach. Several investigations on RIF-SLNs have been reported;[7,13] however, no researchers have ever tried to comprehend the formulation process variables influencing the formulation aspects, through an experimental approach, which could greatly assist in enhancing quality that could help to improve the bioavailability and to reduce its toxicity.

MATERIALS AND METHODS

Materials

RIF was received from Cadila Pharmaceuticals Ltd. India. The Soya Lecithin (LEC), stearic acids (SAs), and Poloxamer-188 (POL) were purchased from HiMedia (Mumbai, India). Remaining all chemicals consumed were of analytical quality.

Experimental design

The QbD of 2^3 factorial designs was applied to assess the effects of three independent parameters and their consequences on the physicochemical property of SLNs. During the optimization of SLNs, the % SA (A), % LEC (B), and % POL (C) were chosen as independent parameters, while the particle size (PS), % of entrapment efficiency (%EE), and % cumulative drug release (%CDR) were considered as dependent (response) parameters. Each one independent factor was set with its low and high levels, as illustrated in Table 1. A total of eight preparations of SLNs (F1–F8) were developed in compliance with the factorial design. The Design Expert Software 10 (Stat-Ease Inc., USA) was employed to analyze the obtained data for evaluating the process variables influencing the formulation aspects and for screening optimized formulation through an experimental approach. It is a valuable tool, which varies each variable simultaneously and gives all possible optimum selections.

Preparation of SLNs

SLNs were fabricated by high-pressure homogenization, followed by ultrasonication technique. In a few words, the lipids (SA and LEC) were melted at a temperature above 10°C of their melting temperature. An aqueous phase was formulated by taking surfactants (POL) and drug in triple distilled water and heated up to the same temperature as that of the lipid phase. Later, the aqueous phase was mixed to the lipid phase, and then the resulting mixture was homogenized at 750 bar and three cycles by employing high-pressure homogenizer (APV 2000, Rosista GmbH). Sonication (Ultrasonicator 300V/T, Biologics, Inc.) for 60 s at 40 pulses was carried out immediately after completion of homogenization. Afterword, the resulting dispersion systems were kept in ice baths for solidification. The SLNs were then collected and were lyophilized to evade sequence of stability issues such as aggregation, fusion, and discharge of the encapsulated drug into the storage medium. The detail composition of SLNs is mentioned in Table 1.

Characterization of SLNs

PS and polydispersity index (PDI)

The 90s Plus PS analyzer with a dynamic laser light scattering technique (Horiba, SZ-100 Scientific series, Japan) was

Table 1: 2^3 Full-factorial design and characterization of prepared RIF-SLNs (Mean [n=3])

FC	SA% (A)	LEC% (B)	POL %(C)	PS*	PDI	ZP (mV)	%TDC	%EE*	%CDR*
F_1	−1	−1	−1	180.6	0.215	−23.3	93.25	64.97	57.39
F_2	−1	+1	−1	202.9	0.238	−26.7	90.32	69.12	51.23
F_3	+1	+1	+1	191.8	0.195	−23.8	92.58	72.45	56.4
F_4	+1	−1	+1	172.5	0.178	−25.6	92.67	70.34	64.34
F_5	+1	−1	−1	198.3	0.208	−24.5	90.12	73.56	54.26
F_6	−1	−1	+1	153.6	0.247	−27.9	91.46	62.54	61.27
F_7	−1	+1	+1	176.7	0.184	−26.5	92.73	66.45	56.34
F_8	+1	+1	−1	212.7	0.275	−27.4	92.87	76.15	48.43

A: -1=1%, +1=2%; B: -1=0.5%, +1=1%; C: -1=1%, +1=2%. FC: Formulation code, LEC: Soya lecithin, SA: Stearic acid, POL; Poloxamer 188, PS: Particle size, PDI: Polydispersity index, ZP: Zeta potential, EE: Entrapment efficiency, TDC: Total drug content, CDR: Cumulative drug release. *Chosen for optimization. RIF: Rifampicin, SLNs: Solid lipid nanoparticle

employed in SLNs dispersions for determining the mean PS and PDI. The dispersions were diluted up to 100 times using deionized water, and then the PS and PDI were measured an angle of 90°.

Zeta potential (ZP)

Horiba, SZ-100 Scientific series, Japan was employed for the determination of the ZP of different formulations with the help of a laser light scattering technique. Double distilled water was used to dilute the formulations appropriately. Measurements were obtained with an angle of 90°.

Total drug content (TDC), %EE

The total quantity of drug per unit volume present in the RIF-SLNs was estimated by suitably disrupting 1 ml of the SLN dispersion in 5 ml chloroform:methanol (1:1) volumetrically. The amount of RIF was determined by UV-visible spectrophotometer at 475 nm. The RIF unloaded SLNs (blank SLNs) prepared in a similar method was considered as control. Each experiment was carried out in triplicate. The following equation was used to estimate the TDC.

$$TDC = \frac{\text{Calculated amount of drug/ml of SLN dispersion}}{\text{Total amount of drug added/ml of SLN dispersion}} \quad (1)$$

The SLN dispersion was undergone centrifugation using Remi cooling centrifuge (Mumbai) for obtaining the clear supernatants that needed for estimation of EE. The following equation was used to estimate the EE.

$$\%EE = \frac{TDC - D_f}{TDC} \times 100 \quad (2)$$

Where D_f = amount of drug in clear supernatant fluid.

In vitro drug release studies

The dialysis bag diffusion method was used for *in vitro* drug release study of RIF-SLNs. Both ends of the dialysis bag (Sigma Laboratories, Osterode, Germany) were clamped after placing 10 ml of SLNs dispersion in it. The bag so formed was engrossed in a receptor compartment containing 200 ml of dissolution media (phosphate buffer of pH 7.4) maintained at 37 ± 0.5°C. A thermostatic shaker (Unimax 1010, Heidolph Instruments GmbH & Co. Schwabach, Germany) at 37°C and rate of 50RPM was used to imitate physiological condition. Five milliliters aliquots were withdrawn at specified time intervals (1, 2, 3, 4, 6, 8, 10, 12, 18, 24, 48, 72, and 96 h) and replaced with an equivalent volume of fresh dissolution medium for maintaining the sink condition. The drug concentration was measured by a UV-visible spectrophotometer at 475 nm by appropriately diluting each withdrawn sample. The %CDR from the different formulations was calculated. The experiments were conducted thrice.

Selection of an optimized formulation

A three-factor, two-level QbD was used to optimize the encapsulation of RIF in the solid lipid matrix. The design setup consisted of eight experimental points. Preliminary trial batches of formulations were developed by considering the extreme values of formulation process variables for getting the preferred formulation with small PS, high %EE, and %CDR. From the preliminary experiments, it was found that the formulation variables such as SA (%), LEC (%), and POL (%) were the key factors that influenced the PS, %EE, and %CDR. Thus, the influence of these three critical, independent formulation variables [A= SA (%), B = LEC (%) and C = POL (%)] on PS, %EE, and %CDR of the prepared SLNs were systemically investigated. The actual values of each variable were coded at two levels for analysis [Table 1]. The response variables such as PS, %EE, and %CDR were analyzed for all the eight experimental points. Analysis of variance (ANOVA) was done, to test the lack of fit and the significance of the linear and interaction effects of the variables on the quality parameters. The F-value in ANOVA is the ratio between the mean square due to regression and the mean square due to real error. Design Expert Statistical

Software Version 10 trial version was used to perform statistical analysis.

Second-order polynomial equation of RSM was applied to optimize the RIF-SLNs considering overall desirability value.[14] A numerical optimization technique was applied to find a point which higher %EE and %CDR, and lower PS. The optimal conditions were selected on the basis of desirability at which experiments were carried out, and the experimental and predicted values were compared to validate the model. To confirm the results, runs were carried out in triplicate under the optimized conditions.

Characterizations of optimized formulation

Scanning electron microscopy (SEM)

Morphology of RIF-SLN was observed using a conventional SEM (JEOL, Japan) at an accelerating voltage of 20 kV. A single drop of RIF-SLNs dispersion was put on the graphite surface. Ion sputter was used for coating the sample with gold after oven-drying.

Fourier transmitter infrared (FTIR) spectroscopy

FT-IR (Agilent Resolution Pro) was employed to record and analyze the IR spectra of pure RIF, SA, and RIF-SLNs, in the range of 4000–600 cm^{-1} at room temperature.

Differential scanning calorimeter (DSC) analysis

The thermal study of RIF, SA, and RIF-SLNs was analyzed using DSC (NETZSCH DSC 214 Polyma, Germany). About 10 mg of samples was placed in aluminum crimp cells and heated from 20 to 300°C with a scanning rate of 10°C/min in a nitrogen ambiance.

The following equation was used for the estimation of % crystallinity indexes (CI %).

$$CI\% = \frac{Enthalpy\,SLNs\,dispersion\,(mj/mg)}{Enthalpy\,bulk\,materials\,(mj/mg)\times Concentration\,lipid\,phase\,(\%)}\times100 \qquad (3)$$

X-ray diffraction (XRD)

The crystal behavior of SLNs was corroborated through XRD study using X-ray diffractometer (XPERT-PRO, PANalytical, the Netherlands). The samples were exposed to Cu K$_\alpha$ radiation (45 kV, 40 mA) and scanned from 10° to 90°, 2θ at a step size of 0.010°. The instrument measures the scattering angle "θ" that helps in calculating the interlayer spacing "d" value using Bragg's equation nλ = 2d sin θ, where "n" is the order of the interference and "λ" is the incident X-ray beam wavelength. A comparison between characteristic peak intensity of pure drug and obtained XRD pattern was done.

Stability studies

Stability study of the freshly prepared lyophilized optimized RIF-SLNs formulations was carried out by keeping sealed vials containing SLNs in a stability chamber maintained at 4 ± 2°C and 25 ± 2°C/60 ± 5% RH. Sealed SLNs were evaluated for PS, %EE over a period of 6 months with sampling at 1, 2, 3, and 6 months.[15]

Statistical analysis

In the present study, all data were reported as the mean ± standard deviation. The significance of differences was evaluated using Student's *t*-test and one-way ANOVA at $P < 0.05$.

RESULTS AND DISCUSSION

Optimization of formulations

RSM was employed for the optimization of RIF-SLNs. The predicted values were estimated through the model fitting technique and found to be sufficiently correlated with the actual values. The actual values were fitted to regression models after meticulous analysis. In fact, fitted response surface without checking the adequacy for the model may provide poor and defective results.[16] Hence, checking of model adequacy is necessary. The decision on the adequacy of models among numerous models representing response parameters of RIF-SLNs was taken by performing the chronological model sum of squares and model summary statistics.[17] The chronological model sum of square has maximum "predicted R^2" and "adjusted R^2" values and had indicated $P < 0.01$ for a quadratic model; therefore, the quadratic model was selected for further analysis.

Results revealed that the PS values varied from 153.6 to 212.7 nm, the %EE varied from 62.54% to 76.15%, and %CDR varied from 48.43% to 64.34%. For obtaining the pragmatic relationship between the experimental results based QbD, the following polynomial equations (second-order) in terms of coded units were generated (Eq^n 4-6).

PS (nm) = +186.14 + 7.69A + 9.89B − 12.49C − 1.46AB + 0.81AC   (4)

%EE = + 69.45 + 3.68A + 1.60B − 1.50C − 0.42AB − 0.23AC − 0.090BC   (5)

%CDR = +56.21 − 3.11B + 3.38C − 0.33AB + 1.13AC − 0.42ABC   (6)

From the polynomial equations, the overall desirability values for all formulations were calculated and found highest (0.91) with the F4 formulation (SA = 2%, LEC = 0.5%, POL = 2%). Thus, F4 formulation was considered as an

optimized formulation. The ANOVA results and statistical parameters for the QbD are shown in Table 2. The model is highly significant as evident from F-test value being 163.88, 3437.37, and 67.31 for PS, %EE, and %CDR, respectively, with $P < 0.05$.

The coefficient of determination (R^2 value) is the best measure of the degree of fit, for PS, %EE, and %CDR were 0.9976, 0.9998, and 0.9941, respectively, and the corresponding adjusted R^2 values were 0.9915, 0.9997, and 0.9793, respectively. In general, the higher the coefficient of variation (CV) value, the lower is the reliability of the experiment. In the present design, the CV value was low (0.94, 0.12, and 1.31) that corroborated a higher level of reliability of the experiments performed.[18] It is implied from very lower value of $P < 0.05$ and higher R^2 value that the selected model is highly significant and sufficient to represent the relationship between the response and independent variables.

Source	Sum of squares	df	Mean square	F-value	P-value Prob. >F	Model
Table 2: ANOVA results and statistical parameters of the QbD model						
PS (nm)						
Model	2524.78	5	504.96	163.88	0.0061	Significant
A-SA	472.78	1	472.78	53.44	0.0065	
B-Lecithin	782.10	1	782.10	253.83	0.0039	
C-POL 188	1247.50	1	1247.50	404.87	0.0025	
AB	17.11	1	17.11	5.55	0.0326	
AC	5.28	1	5.28	1.71	0.0432	
Residual	6.16	2	3.08			
Cor total	2530.94	7				
Std. Dev. 1.76 Mean 186.14 C.V. % 0.94			R-squared 0.9976 Adj. R-squared 0.9915 Pred. R-squared 0.9610			
EE (%)						
Model	148.49	6	24.75	3437.37	0.0131	Significant
A-SA	108.19	1	108.19	15026.67	0.0052	
B-Lecithin	20.35	1	20.35	2826.69	0.0120	
C-POL 188	18.06	1	18.06	2508.34	0.0127	
AB	1.41	1	1.41	196.00	0.0254	
AC	0.41	1	0.41	57.51	0.0335	
BC	0.065	1	0.065	9.00	0.0482	
Residual	0.0072	1	0.0072			
Cor total	148.50	7				
Std. Dev. 0.085 Mean 69.45 C.V. % 0.12			R-squared 0.9998 Adj. R-squared 0.9997 Pred. R-squared 0.9969			
CDR (%)						
Model	181.20	5	36.24	67.31	0.0147	Significant
B-Lecithin	77.25	1	77.25	143.49	0.0069	
C-POL 188	91.40	1	91.40	169.75	0.0058	
AB	0.90	1	0.90	1.67	0.0325	
AC	10.26	1	10.26	19.06	0.0487	
ABC	1.39	1	1.39	2.59	0.0248	
Residual	1.08	2	0.54			
Cor total	182.28	7				
Std. Dev. 0.73 Mean 56.21 C.V. % 1.31			R-squared 0.9941 Adj. R-squared 0.9793 Pred. R-squared 0.9055			

ANOVA: Analysis of variance, SA: Stearic acid, QbD: Quality by design, POL: Poloxamer

To facilitate validation of the predictive ability for each response of the hypothesized model, the optimized form of RIF-SLN was predicted to yield R1 (PS), R2 (%EE), and R3 (%CDR) values of 176.87 nm, 71.75, and 62.68, respectively, when A (%SA), B (%LEC), and C (%POL) values were 2%, 0.5%, and 2%. A new RIF-SLN was prepared with these levels of the independent variables, which yielded the R1 (PS), R2 (%EE), and R3 (%CDR) values of 175.25 nm, 72.17%, and 63.12%, respectively. From the result of each response parameter of the final formulation [Table 3], it was found that the actual values of each response were much closer to the value of the prediction with a low bias percentage. It was also revealed that the optimized form of RIF-SLN (F4) was reliable and prudent as it showed the highest desirability (0.91) value for the formulation.

Table 3: Comparisons between actual values and predicted values of the final formulation under optimized conditions

Response	Predicted values	Actual values	%Bias
R1	176.87	175.25	0.91
R2	71.75	72.17	0.58
R3	62.68	63.12	0.7

R1 = PS (nm), R2 = EE (%), R3 = CDR (%); Bias= (Predicted value-Experimental value)/Predicted value ×100; Acceptance criteria for % Bias =6%. CDR: Cumulative drug release

Effect of process parameters on the response variable

Effect on PS

PS is one of the principal characteristics of the nanoparticles influencing both the release pattern of the drug and its absorption. The response coefficients of each dependent variable were found out to access the effect of each response. The effects of the independent variables such as %SA, %LEC, and %POL concentrations on PS were studied [Figure 1]. The result showed that %SA and %LEC were critical parameters in governing the PS. The mean PS of the prepared SLNs was found lowest with a higher level of POL and lower level of SA and LEC whereas the highest PS of the SLNs was found when SA and LEC were at higher level and POL was at the lower level. Consequently, on increasing the %POL in the lipid matrix from 1% to 2%, the mean PS decreased.

With the increase in the lipid concentration, the PSs of RIF SLNs were increased as the higher tendency of lipid coalescence occurs at higher lipid concentration due to the difference in density between internal and external phases[19] that could be explained by Stokes' law. At high concentration, the viscosity of lipid increases, which leads to reducing the diffusion rate of the solute molecule into the outer phase resulting in increased PS.[20] Moreover, with the increase in the LEC, the size of the SLNs decreases.[15] The PS was
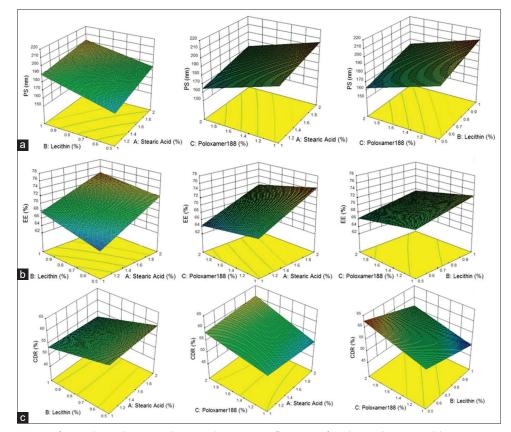

Figure 1: Response surface plots showing the simultaneous influence of independent variables on response parameters (a) particle size, (b) %EE, and (c) % cumulative drug release of rifampicin-solid lipid nanoparticles within the experimental design

decreased on increasing the concentration of POL.[21] It could be elucidated by the dropping of the interfacial tension between the aqueous phase and oily phase by the surfactant that results in the formation of the smaller size of the emulsion droplet.[15] However, the added surfactant helps not only to stabilize the newly formed surfaces but also to avoid the aggregation of particles.[22]

Effect on %EE

An imperative matter regarding the utilization of lipid nanoparticles as drug carriers is their aptitude for EE, and thus the effects on response variable by the independent factors such as the % of POL, %SA, and %LEC were investigated [Figure 1], and the response coefficient for each dependent variable was estimated. The polynomial equation (5) was used for the estimation of %EE of SLNs.

All independent variables showed significant and indirect correlation with EE. With the increase in the level of lipid (%SA), the %EE increases as the higher concentration of lipid leads to the formation of bigger size SLNs particles, which provide some additional space to entrap the drug molecules.[15,19] Higher %EE was obtained at the higher level of LEC due to the higher surfactant behavior of LEC, leading to higher incorporation of drug into the lipid matrix.[15,23] A higher level of POL results in lower %EE value, which may be due to the higher influence of surfactant behavior.[15,24]

Effect on %CDR

The consequence of the independent variables on %CDR in 96 h was studied [Figure 1]. The response coefficients were determined for each dependent variable with a view to evaluating the effect of each response. The %CDR of SLNs was estimated using the polynomial equation (6). The LEC concentration and concentration of POL showed a positive effect on %CDR, whereas an increase in the concentration of SA showed a negative effect on %CDR. The results displayed the highest %CDR (64.34%) at 96 h with the formulation F4 using LEC at the low level and SA and POL at the high level.

Characterization

PS, PDI, and ZP

The PS, PDI, and ZP values of RIF-SLNs are depicted in Table 1.

PS is one of the principal characteristics of the nanoparticles, disturbing both the release pattern of the drug and its absorption. SLNs prepared by our described method were relatively smaller in PS. In general, TB therapy through nanomedicine smaller particles (below 200 nm) are preferred as these not only remain undetectable to the reticuloendothelial system (RES) but also suitable for uptake by the macrophage and for circulation over a protracted episode of time.[15,25] We were successful in getting all PS below 200 nm (mean

PSs range between 153.6 and 212.7 nm). The optimized formulation (F4) showed PS of 172.5 nm.

The PDIs for all the developed systems were between 0.178 and 0.275, indicating a narrow PS distribution. As depicted in Table 1, the ZP values closely ranged between −23.3 mV and −27.9 mV. The least value of ZP was associated with F1 and the highest with F6 and remaining all formulations showed intermediate values. The optimized formulation (F4) showed a ZP value of −25.6mV.

For the development of a production process for a formulation, high recovery of the drug is very much essential as it accounts for losses of the drug during the process. For our formulation, we have achieved >90% TDC values, which signifies the suitability of the developed process and its scale-up applicability. The PDIs of all the developed SLNs systems were <0.3, which indicates a narrow and homogeneous PS distribution.

The nanoparticles are thermodynamically unstable systems and a ZP value of equal to or more than −30 mV is desirable for the stability of colloidal drug carriers. ZP values of all prepared formulations were found to be significantly negative ($P < 0.05$) and predict high particle stability and limit aggregation with prolonged storage. LEC and POL are the main components in formulations that influence the ZP. The negatively charged value of ZP may be ascribed by the LEC, which is an anionic surfactant that caused electrostatic repulsion among the particles ensuing in a reduction in the aggregation of particles.[26] The ZP of formulations decreases with an increase in LEC. Moreover, on an increase in % POL, the ZP value decreases as POL is a non-ionic surfactant.

EE and TDC

Highest %EE (76.15%) was observed with a high level of SA, LEC, and low level of POL concentrations whereas lowest %EE (62.54%) was obtained with higher POL concentration and low level of LEC and SA. The optimized formulation (F4) showed a %EE of 70.34%.

All the SLN formulations exhibited a TDC of > 90% w/v.

In vitro drug release studies and release kinetics

The %CDR was found to range from 48.43 to 64.34% up to 96 h depending on the independent variables. Highest %CDR (64.34%) was observed with a higher level of POL and SA and lower levels of LEC. However, the lowest %CDR (48.43%) was observed at a higher level of SA and LEC but at a lower level of POL.

In an attempt to develop an extended-release system, it is imperative to be aware of the release mechanism and kinetics. The drug release profiles of RIF SLNs were biphasic pattern in which initially faster drug release phase (burst effect)

until 12 h subsequently by a slower controlled drug release phase [Figure 2]. The burst effect may be attributed to the unbound drug and the drug molecules that adsorbed on the SLNs surface.[21,22] The controlled release pattern depends on the rate of release of the entrapped RIF that further depends on the degree of solubility and rate of diffusion of RIF from the lipid matrix. The diffusion of RIF from lipid matrix also depends on the partitioning of RIF between the lipid phase and the aqueous dissolution media.

The *in vitro* drug release data from RIF SLNs were fitted into zero-order, first-order, Higuchi, and Korsmeyer–Peppas model to study the drug release characteristics. The drug release kinetics data are shown in Table 4. On comparing the R^2 values of the SLNs, it was proved that it followed Higuchi and Korsmeyer–Peppas equations. However, it was best fitted to Higuchi model. The release exponent "n" is greater than 0.5, which implies that the mechanism of release of RIF from SLN was non-Fickan diffusion. For the optimized formulation, 51% of the drug was released at the end of 12 h, and after about 96 h, drug release reached a steady state (79%). This validates that the prepared RIF-SLN can sustain the drug release into the systemic circulation, and hypothetically may be able to lower dosing frequency.

SEM

From the SEM images [Figure 3], it was observed that the developed SLNs were spherical in shape having nanometer size. Moreover, it also observed through both SEM and dynamic light scattering technique that the size of the SLNs particles was in a good agreement.

FTIR studies

FTIR spectra of RIF [Figure 4] showed that characteristic peaks at 3425.7 cm^{-1} belong to –OH stretching, 2934 cm^{-1} belong to –NH stretching, 1730 cm^{-1} belong to -C=O stretching, 1644 cm^{-1} belong to -CONH$_2$ stretching, and 1236 cm^{-1} belong to -C-O-C- stretching. FTIR spectrum

Figure 2: *In vitro* release profiles of rifampicin-solid lipid nanoparticles up to 96 h F1–F8 in phosphate buffer, pH 7.4
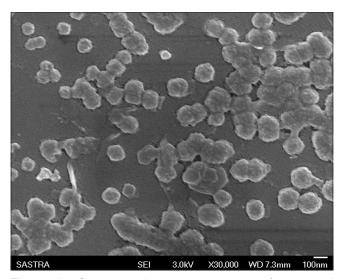

Figure 3: Scanning electron microscopy of optimized rifampicin-solid lipid nanoparticles (F4)

FC	Zero order		First order		Higuchi		Korsmeyer-Peppas		
	K_0	R^2	K_1	R^2	K_h	R^2	n	K_p	R^2
F1	0.57	0.817	0.006	0.896	6.36	0.962	0.591	5.09	0.948
F2	0.52	0.831	0.006	0.88	5.8	0.964	0.611	4.04	0.968
F3	0.56	0.817	0.006	0.891	6.32	0.961	0.601	3.99	0.954
F4	0.59	0.772	0.006	0.89	6.75	0.942	0.509	7.88	0.943
F5	0.54	0.813	0.009	0.883	6.02	0.955	0.584	4.82	0.965
F6	0.58	0.79	0.009	0.876	6.56	0.951	0.55	6.45	0.935
F7	0.56	0.832	0.006	0.902	6.31	0.968	0.603	4.73	0.954
F8	0.5	0.837	0.006	0.89	5.59	0.955	0.706	2.6	0.95

Table 4: *In vitro* release kinetics of RIF- SLNs formulations up to 96 h
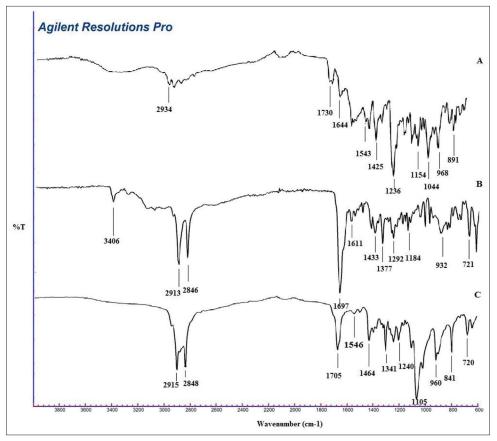
Figure 4: FTIR spectrum of (A) free rifampicin (RIF), (B) stearic acid, and (C) RIF-solid lipid nanoparticles (F4)
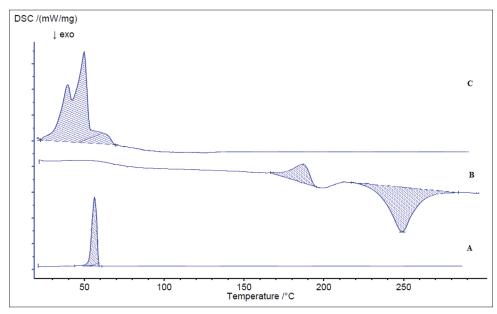

Figure 5: DSC thermograms of (A) stearic acid; (B) rifampicin (RIF), and (C) RIF-solid lipid nanoparticles (F4)

of SA showed that 3406 cm^{-1} belongs to C-H stretching, 2913 cm^{-1} and 2846 cm^{-1} belong to O-H stretching, 1697 cm^{-1} belongs to C=0 stretching, and 1433 cm^{-1} belongs to C=C stretching. The characteristic FTIR peaks of RIF and SA were present in RIF-SLNs. This confirms that RIF was compatible with SA and was remained stable during SLNs formulation.

DSC studies

The DSC thermograms of pure RIF, SA, and RIF-SLNs are shown in Figure 5. The pure RIF showed a single sharp exothermic peak at about 250.2°C (ΔH = −126.1 J/g) and endothermic peak at about 187.7°C (ΔH = 34.91 J/g) whereas SA showed an endothermic peak at 56.3°C (ΔH = 194.4 J/g).

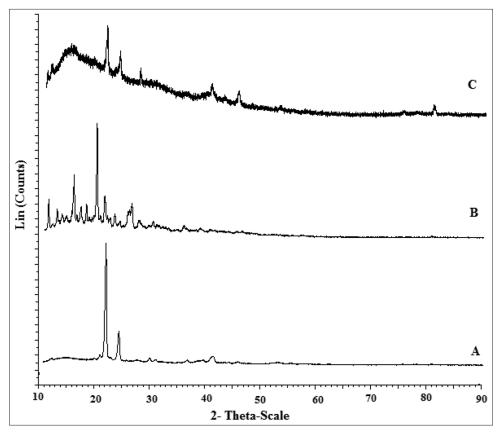**Figure 6:** X-ray diffraction spectrums of (A) stearic acid, (B) rifampicin (RIF), (C) RIF-solid lipid nanoparticles (F4).

Table 5: Stability study of freeze-dried RIF-SLN formulation for PS and %EE assessment over 6 months

Time (month)	PS (nm)		% Entrapment Efficiency	
	4±2°C	25±2°C, 60±5% RH	4±2°C	25±2°C, 60±5% RH
0	172.5±3.14	172.5±3.14	70.34±1.97	70.34±1.97
1	174.7±2.95	177.3±1.32	69.81±2.37	68.21±2.10
2	178.5±2.73	183.6±2.11	68.14±0.97	67.22±1.39
3	182.3±2.91	188.2±1.78	67.1±1.17	65.34±1.77
6	188.6±1.76	197.3±2.65	65.67±2.37	61.33±2.12

RIF: Rifampicin, SLN: Solid lipid nanoparticle, PS: Particle size, %EE: % Entrapment efficiency

In the DSC thermogram of RIF-SLNs, the depressed endothermic peak with a significant decrease in enthalpy of the peak was observed at 51.6°C (180.6 J/g). However, the RIF peak was not visible in the SLNs thermogram. It signified that the RIF was molecularly dispersed homogeneously in the nanoparticulate matrix system and was not in a crystalline form. The nanometric PS, enormous surface area, and effect of surfactant were believed to be responsible for the depressed endothermic peak. A reduction in the crystallinity should be maintained during the preparation of RIF SLNs to keep the drug molecules within the solid lipid corpse. The % CI of the optimized RIF SLNs was calculated and found to be 46.45% against the reference value of 100% for SA. It was validated that on addition of LEC and POL, the recrystallization tendency of solid lipid reduced due to the depression of the crystallinity that responsible for promoting more disordered arrangement.

It was concluded from DSC studies that for monitoring the drug loading, the solubility of RIF in lipid, and the presence of lipid imperfection were two important factors. In this study, the results were validated for a drop off in enthalpy change that correlated with the generation of imperfections (loss of crystallinity) indicating successful accommodation of the drug molecule within the lipid crystals ensuring expulsion of the drug in minimum quantity and controlled release of drug from the RIF SLNs with a minimum burst effect.[22]

XRD

XRD patterns of RIF, SA, and RIF-SLN are shown in Figure 6. XRD pattern of RIF exhibited characteristic peaks between 2θ scattered angles of 10° and 25° indicating a crystalline

nature. In the XRD pattern of lyophilized RIF-SLNs, it was marked that the major characteristic peaks of RIF disappeared, indicating its large amorphousness on incorporation into the lipid matrix. However, the peaks obtained from the XRD of lyophilized RIF-SLNs were blurred, broad, and diffuse with low intensities along with some pure drug corresponding peaks. The reason of presence of low intensities peaks corresponding to pure drugs may be ascribed to the presence of free drugs in the formulation. The faster dissolving rate of amorphous or metastable form of RIF in lipid is due to its higher internal energy that enhances thermodynamic characteristics when compared to crystalline materials. The extent of drug encapsulation and rate of drug release depend on the polymorphic behavior and crystallinity of SLNs which could be modified by the presence of surfactants, method of fabrication, and size.

Stability studies

The stability of optimized lyophilized formulation was investigated at different temperature and conditions (at $4 \pm 2°C$ and $25 \pm 2°C$, $60 \pm 5\%$ RH) and the observed data are shown in Table 5. The mean diameters of RIF-SLNs were increased from 172.5 to 188.6 nm at $5 \pm 3°C$ whereas it was increased up to 197.3 nm at $25 \pm 2°C$, $60 \pm 5\%$ RH after 6 months study period. The %EE was reduced by 4.67% at $4 \pm 2°C$ whereas it was reduced by 9.01% at $25 \pm 2°C$, $60 \pm 5\%$ RH after 6 months of storage. Stability study indicated that at both the temperature RIF-SLNs showed good stability, though there was a decrease in %EE and increase in PS. Comparatively higher reduction of %EE of lyophilized RIF-SLNs at $25 \pm 2°C$, $60 \pm 5\%$ RH as compared to $4 \pm 2°C$. The higher amount of RIF expulsion from the RIF-SLNs at $25 \pm 2°C$ could be explained by the higher fluidity of lipid at the higher temperature. Smaller PS is responsible for transitions of SA from metastable forms to stable forms slowly during storage, and the presence of surfactants may also be the reason for drug expulsion from SLNs.

CONCLUSIONS

The formulation process variables of RIF-SLNs were optimized by QbD of RSM. To validate the model, actual and predicted values of the responses at optimized conditions were processed, and the results indicate that the difference between predicted value generated and actual value measured was not significant, confirming the reliability of the model. Moreover, in this study, RIF-SLNs having nano PS with improved %EE were successfully prepared. The nano-size particles were suitable for bypassing RES and thereby may prevent first-pass metabolism. The *in vitro* drug release kinetics revealed that the release of RIF from the SLNs followed non-Fickian's mechanism. The burst release of RIF at the initial stage may help in achieving minimum therapeutic concentration, and the secondary controlled release characteristic helps in maintaining the therapeutic concentration.

Thus, SLNs could be used for delivery of RIF to achieve controlled release of drug in systemic circulation that may improve bioavailability and reduce toxicity for effective TB therapy.

REFERENCES

1. Craig GM, Daftary A, Engel N, O'Driscoll S, Ioannaki A. Tuberculosis stigma as a social determinant of health: A systematic mapping review of research in low incidence countries. Int J Infect Dis 2017;56:90-100.
2. World Health Organization. Global Tuberculosis Report 2016. Geneva: Available from: https://www.who.int/tb/publications/factsheet_global.pdf?ua=1
3. Nusrath Unissa A, Hanna LE. Molecular mechanisms of action, resistance, detection to the first-line anti tuberculosis drugs: Rifampicin and pyrazinamide in the post whole genome sequencing era. Tuberculosis (Edinb) 2017;105:96-107.
4. Singh H, Jindal S, Singh M, Sharma G, Kaur IP. Nano-formulation of rifampicin with enhanced bioavailability: Development, characterization and *in vivo* safety. Int J Pharm 2015;485:138-51.
5. Goyal P, Gill S, Gupta UD, Rath G, Narang RK, Goyal AK. Development and characterization of rifampicin loaded floating microspheres. Artif Cells Blood Substit Immobil Biotechnol 2011;39:330-4.
6. Patil JS, Devi VK, Devi K, Sarasija S. A novel approach for lung delivery of rifampicin-loaded liposomes in dry powder form for the treatment of tuberculosis. Lung India 2015;32:331-8.
7. Pooja D, Tunki L, Kulhari H, Reddy BB, Sistla R. Characterization, biorecognitive activity and stability of WGA grafted lipid nanostructures for the controlled delivery of Rifampicin. Chem Phys Lipids 2015;193:11-7.
8. Kakkar V, Singh S, Singla D, Kaur IP. Exploring solid lipid nanoparticles to enhance the oral bioavailability of curcumin. Mol Nutr Food Res 2011;55:495-503.
9. Bibhas CM, Subas CD, Gitanjali M, Narahari NP. Exploring the use of lipid based nano-formulations for the management of tuberculosis. J Nanosci Curr Res 2017;2:1-15.
10. Smith I. *Mycobacterium tuberculosis* pathogenesis and molecular determinants of virulence. Clin Microbiol Rev 2003;16:463-96.
11. Kaur IP, Singh H. Nanostructured drug delivery for better management of tuberculosis. J Control Release 2014;184:36-50.
12. Sangshetti JN, Deshpande M, Zaheer Z, Shinde DB,

Arote R. Quality by design approach: Regulatory need. Arab J Chem 2017;10:S3412-25.

13. Song X, Lin Q, Guo L, Fu Y, Han J, Ke H, *et al*. Rifampicin loaded mannosylated cationic nanostructured lipid carriers for alveolar macrophage-specific delivery. Pharm Res 2015;32:1741-51.

14. Wei Z, Hao J, Yuan S, Li Y, Juan W, Sha X, *et al*. Paclitaxel-loaded pluronic P123/F127 mixed polymeric micelles: Formulation, optimization and *in vitro* characterization. Int J Pharm 2009;376:176-85.

15. Mohanta BC, Dinda SC, Mishra G, Palei NN, Dusthackeer VN. Formulation, characterization, *in vitro* anti-tubercular activity and cytotoxicity study of solid lipid nanoparticles of Isoniazid. Nano Biomed Eng 2018;10:379-91.

16. Omwamba M, Hu Q. Antioxidant capacity and antioxidative compounds in barley (*Hordeum vulgare* L.) grain optimized using response surface methodology in hot air roasting. Eur Food Res Technol 2009;229:907-14.

17. Maran JP, Sivakumar V, Sridhar R, Thirugnanasambandham K. Development of model for barrier and optical properties of jackfruit seed starch based films. Carbohydr Polym 2013;92:1335-47.

18. Li Y, Liu Z, Zhao H, Xu Y, Cui F. Statistical optimization of xylanase production from new isolated *Penicillium oxalicum* ZH-30 in submerged fermentation. Biochem Eng J 2007;34:82-6.

19. Palei NN, Das MK. Formulation, optimization and evaluation of solid lipid nanoparticles of lornoxicam. Lat Am J Pharm 2013;32:1528-37.

20. Ruckmani K, Sivakumar M, Ganeshkumar PA. Methotrexate loaded solid lipid nanoparticles (SLN) for effective treatment of carcinoma. J Nanosci Nanotechnol 2006;6:2991-5.

21. Sanjula B, Shah FM, Javed A, Alka A. Effect of poloxamer 188 on lymphatic uptake of carvedilol-loaded solid lipid nanoparticles for bioavailability enhancement. J Drug Target 2009;17:249-56.

22. Palei NN, Mohanta BC, Das MK, Sabapathi ML. Lornoxicam loaded nanostructured lipid carriers for topical delivery: Optimization, skin uptake and *in vivo* studies. J Drug Deliv Sci Technol 2017;39:490-500.

23. Khallaf RA, Salem HF, Abdelbary A. 5-Fluorouracil shell-enriched solid lipid nanoparticles (SLN) for effective skin carcinoma treatment. Drug Deliv 2016;23:3452-60.

24. Bhalekar M, Upadhaya P, Madgulkar A. Formulation and characterization of solid lipid nanoparticles for an anti-retroviral drug darunavir. Appl Nanosci 2017;7:47-57.

25. Mustafa S, Devi VK, Pai RS. Kanamycin sulphate loaded PLGA-Vitamin-E-TPGS long circulating nanoparticles using combined coating of PEG and water-soluble chitosan. J Drug Deliv 2017;2017:1253294.

26. Shah M, Agrawal YK, Garala K, Ramkishan A. Solid lipid nanoparticles of a water soluble drug, ciprofloxacin hydrochloride. Indian J Pharm Sci 2012;74:434-42.